

An efficient PEGylated liposomal nanocarrier containing cell-penetrating peptide and pH-sensitive hydrazone bond for enhancing tumor-targeted drug delivery

Yuan Ding^{1,*}Dan Sun^{1,*}Gui-Ling Wang¹Hong-Ge Yang¹Hai-Feng Xu¹Jian-Hua Chen²Ying Xie^{1,3}Zhi-Qiang Wang⁴

¹Beijing Key Laboratory of Molecular Pharmaceutics and New Drug Delivery Systems, School of Pharmaceutical Sciences, Peking University, Beijing, ²School of Medicine, Jiangnan University, Wuhan, ³State Key Laboratory of Natural and Biomimetic Drugs, Peking University, Beijing, People's Republic of China; ⁴Department of Chemistry and Biochemistry, Kent State University Geauga, Burton, OH, USA

*These authors contributed equally to this work

Correspondence: Ying Xie
School of Pharmaceutical Sciences, Peking University, 38 Xueyuan Road, Beijing 100191, People's Republic of China
Tel +86 10 8280 1508
Fax +86 10 8280 2745
Email bmuxieying@bjmu.edu.cn

Jian-Hua Chen
School of Medicine, Jiangnan University, Wuhan 430056, People's Republic of China
Tel +86 27 8338 7177
Email jeff5ch@163.com

Abstract: Cell-penetrating peptides (CPPs) as small molecular transporters with abilities of cell penetrating, internalization, and endosomal escape have potential prospect in drug delivery systems. However, a bottleneck hampering their application is the poor specificity for cells. By utilizing the function of hydration shell of polyethylene glycol (PEG) and acid sensitivity of hydrazone bond, we constructed a kind of CPP-modified pH-sensitive PEGylated liposomes (CPPL) to improve the selectivity of these peptides for tumor targeting. In CPPL, CPP was directly attached to liposome surfaces via coupling with stearate (STR) to avoid the hindrance of PEG as a linker on the penetrating efficiency of CPP. A PEG derivative by conjugating PEG with STR via acid-degradable hydrazone bond (PEG2000-Hz-STR, PHS) was synthesized. High-performance liquid chromatography and flow cytometry demonstrated that PHS was stable at normal neutral conditions and PEG could be completely cleaved from liposome surface to expose CPP under acidic environments in tumor. An optimal CPP density on liposomes was screened to guaranty a maximum targeting efficiency on tumor cells as well as not being captured by normal cells that consequently lead to a long circulation in blood. In vitro and in vivo studies indicated, in 4 mol% CPP of lipid modified system, that CPP exerted higher efficiency on internalizing the liposomes into targeted subcellular compartments while remaining inactive and free from opsonins at a maximum extent in systemic circulation. The 4% CPPL as a drug delivery system will have great potential in the clinical application of anticancer drugs in future.

Keywords: long circulation, pharmacokinetics, lysosome escape, nanocarrier, pH-sensitive liposomes

Introduction

Liposomes are widely used as nanocarriers that are capable of loading various cargos and show advantages of biocompatibility, biodegradability, and ease of modification.¹ Currently, intracellular or organelle-specific targeting is becoming an emerging concept for improving the drug action of nanocarriers.^{2,3} Cell-penetrating peptides (CPPs), also known as protein transduction domains, are a class of short peptide sequences that are capable of entering cells efficiently, either alone or linked to bulky cargoes (eg, protein, plasmid DNA, oligonucleotides, and liposomes).^{4,5} Nevertheless, the application of CPPs in drug delivery system (DDS) is limited by its attributes, namely, nonspecificity and enzymatic cleavage.

To overcome these impediments, “smart” DDS was developed, including dual-ligand liposomes conducted by a specific ligand^{6,7} and pH-sensitive liposomes constructed with a degradable polyethylene glycol (PEG) derivative (PEG2000-Hz-PE).⁷

Recent work of PEG2000-Hz-PE conjugate showed that it has a degradation half-time of 3.0 hours at pH 5.5 due to an immediate aromatic ring (electron withdrawing) next to hydrazone bond⁷ (Figure 1D). However, the degradation time is too long compared to the 20 minutes of liposomes distribution in blood.⁸ Such a long degradation time may restrict the exposure of CPP at tumor site. In the current study, we designed a new PEG derivative named PHS (mPEG2000-Hz-STR) (Figure 1A) to expect stronger

pH sensitivity as well as shorter degradation time since methylene group (electron donating) was introduced next to the hydrazone bond.

It is obvious that PEG plays critical roles in improving the selectivity of CPP^{6,7} for both dual-ligand liposomes and pH-sensitive DDS. However, our previous results showed that PEG as a linker played obstructive roles on cellular uptake as well (Supplementary materials). Therefore, attaching CPP directly on liposome surfaces will avoid the

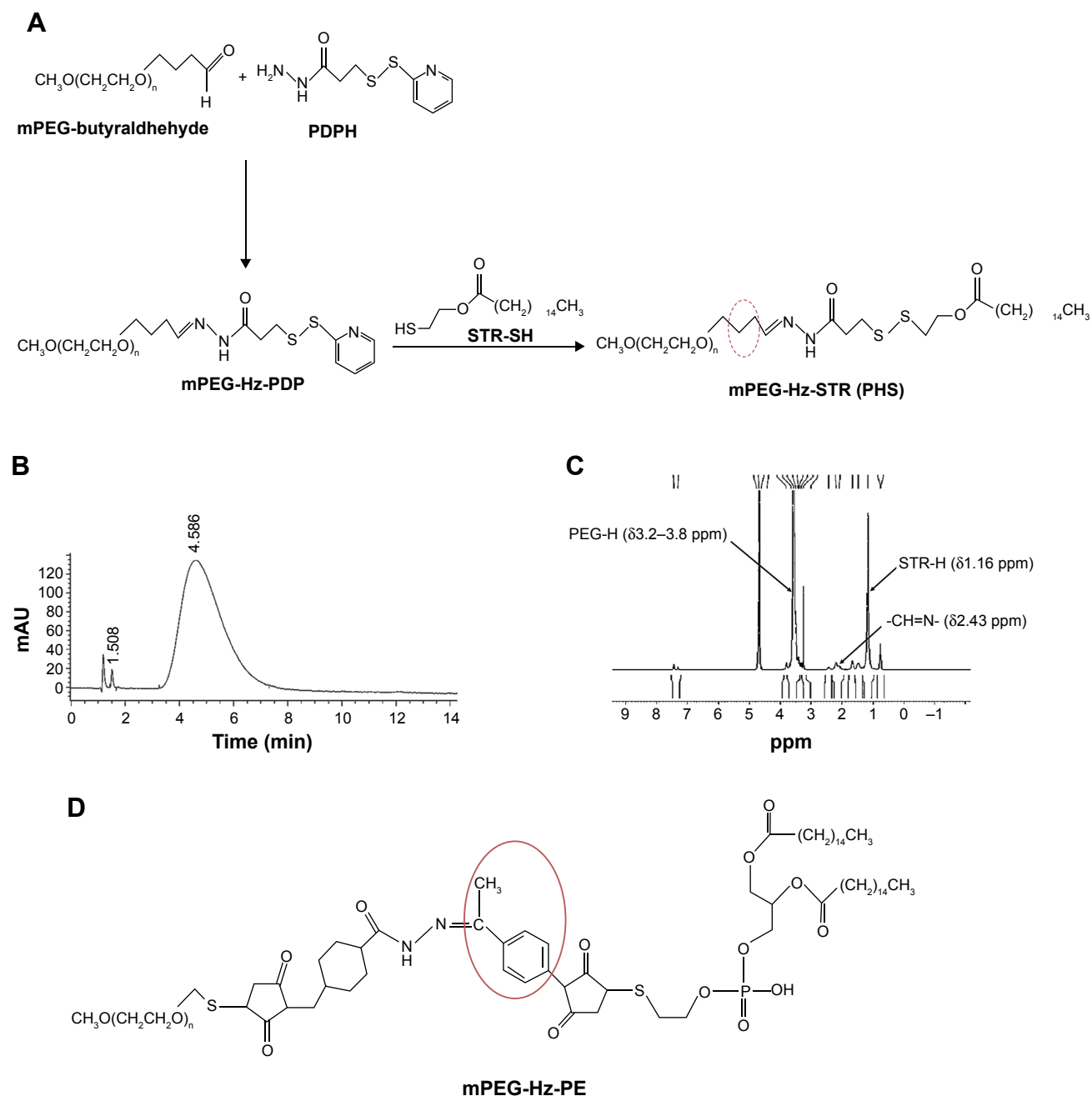


Figure 1 (A) The synthetic route of PHS. (B) HPLC spectrum of PHS. (C) ¹H NMR spectrum of PHS, D₂O was used as a solvent. (D) The chemical structure of mPEG-Hz-PE.

Abbreviations: PHS, mPEG2000-hydrazone-stearate (mPEG2000-Hz-STR); HPLC, high-performance liquid chromatography; PEG, polyethylene glycol; min, minutes.

hindrance of PEG and may become a better strategy for improving the penetrating efficiency of CPP. In addition, it is worthy investigating the maximum density of CPP that could be shielded by PEG in the system to exert CPP maximum targeting efficiency on tumor site, but not to penetrate normal tissues at neutral pH conditions.

In the present study, we introduced a novel pH-sensitive PEG derivative material and designed an efficient CPP-modified, pH-sensitive PEGylated liposomes (CPPL), in which CPP was directly attached on liposome surfaces via coupling with STR, and PHS was incorporated into the liposome membrane to exert dual function at different pH environment. We evaluated pH sensitivity of CPPL and screened modification density of CPP. We expect such a novel and effective CPPL DDS to perform well in prolonged circulation, physical tumor targeting, strong intracellular penetration, as well as efficient endosomal escaping to accomplish nucleus targeting of anticancer drugs.

Materials and methods

Materials

Soybean phosphatidylcholine (SPC, 99% purity) was purchased from Shanghai Taiwei Chemical Company (Shanghai, People's Republic of China). Cholesterol was purchased from Alfa Aesar Co, Ltd (Beijing, People's Republic of China). 1,2-Distearoyl-sn-glycero-3-phosphoethanolamine-*N*-[methoxy(polyethyleneglycol)-2000] (DSPE-PEG2000) was purchased from Shanghai Advanced Vehicle Technology Pharmaceutical, Ltd (Shanghai, People's Republic of China). Stearic (STR) was obtained from Beijing Chemical Factory (Beijing, People's Republic of China). 1-(3-Dimethylaminopropyl)-3-ethylcarbodiimide hydrochloride (EDCI) was obtained from J&K Scientific, Ltd (Hong Kong, People's Republic of China). CPP-FITC (RRRRRRRRRK [β -Ala-FITC]-amide) and CPP (GGRRRRRRRRR-amide) were provided by KTG Pharmaceuticals, Inc. (Wuhan, Hubei province, People's Republic of China). Coumarin-6 and doxorubicin (DOX) were from Sigma-Aldrich Co (St Louis, MO, USA) and Melunbio Co, Ltd (Dalian, Lioing province, People's Republic of China), respectively.

Animals

Male Sprague Dawley rats (200 \pm 20 g) and BALB/c nude mice (20 \pm 2 g) were provided by the Animal Center of Peking University Health Science Center. All procedures involving animal housing and treatment were approved by the Institutional Authority for Laboratory Animal Care of Peking University.

Cell culture

MCF-7 human breast cancer cell line was purchased from the Institute of Basic Medical Science, Chinese Academy of Medical Science (Beijing, People's Republic of China). Cells were cultured in RPMI 1640 containing 2 mM L-glutamine and were supplemented with 10% (v/v) heat-inactivated fetal bovine serum, 100 U/mL penicillin, and 100 μ g/mL streptomycin. Cultures were maintained at 37°C in a humidified 5% CO₂ incubator. The pH of culture medium was adjusted to pH 7.0 or 6.0 with 0.1 mol/L HCl prior to treatments.

Synthesis and characterization of PHS

PHS was synthesized (Figure 1A) based on the method proposed by Kale and Torchilin⁹ with some modifications (Supplementary materials). The structure of PHS was confirmed by high-performance liquid chromatography (HPLC) spectrum (Agilent HP 1100 HPLC/evaporative light scattering detector; Agilent Technologies, Santa Clara, CA, USA) (Figure 1B) and ¹H NMR (AVANCE III, 400 MHz; Bruker Corporation, Billerica, MA, USA) (Figure 1C).

Preparation and characterization of various liposomes including CL, PL, PSL, CPL, and CPPL

CPPL with various CPP densities were prepared using lipid thin film hydration¹⁰ as described in Figure 2. The thin film containing SPC/cholesterol/STR was hydrated with phosphate-buffered saline (PBS, pH 7.0) under sonication at 37°C for 20 minutes to form conventional liposomes (CL). EDCI and S-NHS were added into CL containing STR at STR/EDCI/S-NHS molar ratio of 1:40:100 to activate STR moiety on CL.¹¹ The solution pH was adjusted to 12, and then CPP with an equivalent amount of STR reacted with NHS-activated CL for 12 hours to form CPP-modified conventional liposomes (CCL). The suspension in an ultrafilter tube (MWCO, 30,000 Da) was centrifuged at 1,000 \times g for 30 minutes to remove unreacted EDCI, S-NHS, and CPP. To obtain CPPL, 8 mol% PHS of SPC was incubated with CCL at pH 7.0 for 12 hours. CPP-modified PEGylated liposomes (CPL) were prepared with similar method except substituting PHS with DSPE-PEG. PEGylated liposomes (PL) and pH-sensitive PEGylated liposomes (PSL) were prepared as controls without CPP modification.

For the investigation of pH sensitivity and optimization of modified density of CPP on CPPL by flow cytometry (FCM), we prepared coumarin-6-loaded liposomes (lipids:coumarin-6 = 2,000:1, w/w) using lipid film hydration

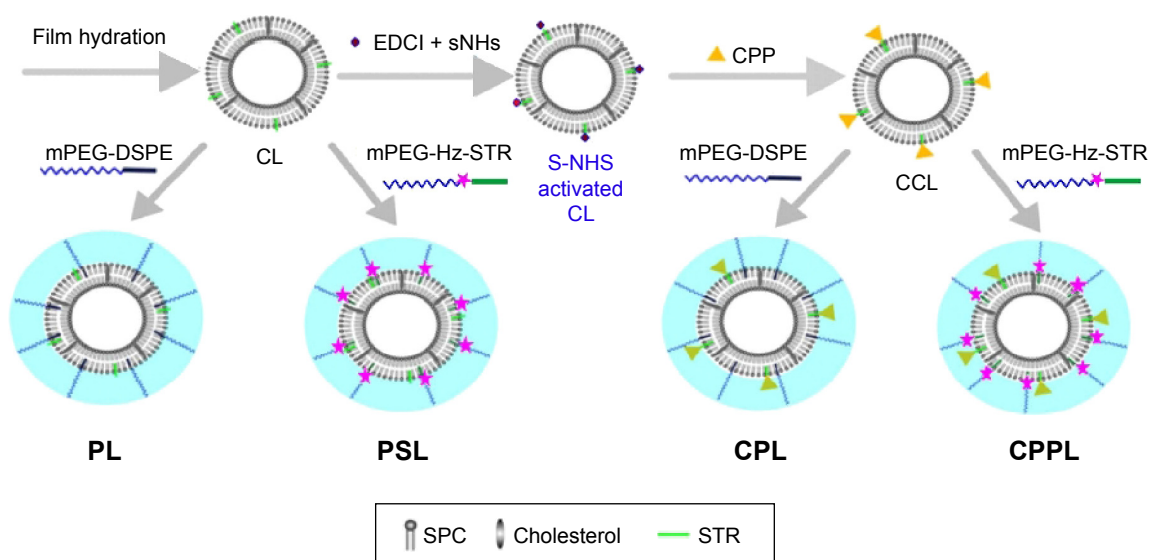


Figure 2 Scheme of various liposomes preparations including CL, CCL, PL, PSL, CPL, and CPPL.

Abbreviations: CL, conventional liposomes; CCL, CPP-modified conventional liposomes; PL, PEGylated liposomes; PSL, pH-sensitive PEGylated liposomes; CPL, CPP-modified PEGylated liposomes; CPPL, CPP-modified pH-sensitive PEGylated liposomes; CPP, cell-penetrating peptide; PEG, polyethylene glycol; SPC, soybean phosphatidylcholine; STR, stearic acid; EDCI, 1-(3-dimethylaminopropyl)-3-ethylcarbodiimide hydrochloride; mPEG, methoxy(polyethyleneglycol); DSPE, 1,2-Distearoyl-sn-glycero-3-phosphoethanolamine.

method as described previously.¹⁰ For confocal images and cytotoxicity studies, DOX was loaded into liposomes by pH-gradient method.¹²

The coupling efficiency (*ce*) of CPP on liposomes was determined using fluorescence spectrometer in conjunction with ultrafiltration method. FITC-CPPL was prepared in a similar way except substituting CPP with CPP-FITC. Free CPP-FITC was separated from CPPL via centrifugation at 1,000×*g* for 30 minutes by an ultrafilter tube (MWCO, 30,000 Da). Fluorescence intensities (FI) of FITC-CPPL suspension before and after centrifugation were measured, respectively, by a fluorescence spectrophotometer (Cary Eclipse, Varian Associates, USA) at λ_{ex} =492 nm and λ_{em} =518 nm. The formula used is $ce = FI \text{ (after)}/FI \text{ (before)} \times 100\%$.

To analyze the changes in size and zeta potential of liposomes caused by 4 mol% CPP modification, PL, CCL, and CPPL (pH 7.0 and incubation at pH 6.0 for 30 minutes) were diluted by distilled water. After filtering each liposome with 0.45 μm filter membrane, size distribution (in nm), polydispersity index, and zeta potential were determined at 25°C using Nano ZS ZEN3600 Zetasizer (Malvern Instruments, Malvern, UK). Assays were run for 15 times with an equilibrium time of 60 seconds.

pH sensitivity of PSL evaluated by HPLC and FCM

HPLC method: The pH sensitivity of liposomes with 8 mol% PHS of SPC insertion was analyzed using size

exclusion chromatography.⁹ PSL were incubated in $(\text{NH}_4)_2\text{CO}_3$ buffers at pH of 7.0, 6.5, 6.0, or 4.5 for 0.5 hour at room temperature. Conjugate degradation was followed by HPLC using a Shodex KW-804 exclusion column (8.0 mm ×300 mm). The mobile phase was deionized water, flow rate was 1.0 mL/min, and the injection volume was 5 μL . The peaks of liposomes and free PEG were detected with Waters 2424 ELS Detector (Waters, USA) under the following conditions: pure nitrogen, drift tube at 80°C, and nitrogen gas pressure at 30 psi. According to the principle of ELSD measurement that the mass of the substance is proportional to its peak area, the relative mass of PEG was calculated as: $m \text{ (PEG)}\% = A \text{ (PEG)}/(A \text{ [PEG]} + A \text{ [liposomes]}) \times 100\%$, where *A* (LSU·min) was the peak area.

FCM method: 1×10^6 cells/well MCF-7 were seeded onto a six-well plate and cultured at 37°C in a humidified 5% CO_2 incubator for 24 hours. Cells were incubated with free serum RPMI 1640 containing coumarin-6-PSL (100 ng/mL coumarin-6) under pH 7.0 and 6.0 for 3 hours, respectively. Cells were then suspended into 0.5 mL PBS and passed through a 300-mesh cell strainer prior to fluorescence-activated cell sorting (FACS) using a FACS Calibur flow cytometer (BD Biosciences, San Jose, CA, USA). Cells were enclosed in a forward versus side scatter gate to exclude debris and dead cells prior to analysis of 10,000 cell counts. Data were analyzed via BD Cell Quest Pro software. PL and CL were served as controls.

Optimizing CPP density in CPPL

MCF-7 cells were incubated with free serum RPMI 1640 containing 100 ng/mL coumarin-6- $x\%$ -CPPL ($x=0, 1, 2, 4,$ and 8) at pH 7.0 and 6.0 for 3 hours, respectively. FI of each sample were measured by a flow meter based on the protocol of FCM as described earlier. The optimized density of CPP in CPPL was determined to be the maximum CPP density that cannot be shielded by PEG on the CPPL uptake by normal or tumor cells at neutral pH.

In vitro confocal image of DOX-CPPL

MCF-7 cells at a density of 2×10^5 cells per dish were cultured onto glass-based dishes for cellular uptake studies of DOX-CPPL at different pH. Cells were rinsed with PBS twice after 24-hour culture and were incubated with DOX-PSL/DOX-CPL/DOX-CCL/DOX-CPPL (containing 20 $\mu\text{g}/\text{mL}$ DOX and 4 mol% CPP of SPC) at pH 6.0 and 7.0 for 2 hours. Cells were then rinsed with PBS and fixed with 4% paraformaldehyde. Cell nuclei were stained with Hoechst 33258, and samples were studied using a Leica TCS SP5 confocal laser-scanning microscope (CLSM, Heidelberg, Germany). The average light intensity of 15 areas was analyzed by ImageJ (Version 1.47, National Institutes of Health, USA).

Time course of cellular uptake of DOX-CPPL was also studied using the above method under pH 6.0/7.0 and various incubation times (2 hours, 4 hours, and 8 hours).

Internalization of coumarin-6-CPPL and coumarin-6-PL

MCF-7 cells were incubated with coumarin-6-CPPL (4 mol% CPP of SPC) or coumarin-6-PL at a final concentration of 100 ng/mL coumarin-6 at pH 6.0 for 2 hours. Cells were rinsed with PBS twice and then incubated with 500 nmol/L LysoTracker Red (Thermo Fisher Scientific, Waltham, MA, USA) for 30 minutes. The internalization and endosomal release of liposomal coumarin-6 were measured using CLSM following 2-hour time period. The LysoTracker Red was excited by a 561 nm laser.

Pharmacokinetics and biodistribution of CPPL in vivo

The $^{99\text{m}}\text{Tc}$ -labeled liposomes were biologically stable^{13,14} and directly reflected the clearance and distribution of the liposomes in various tissues. Pharmacokinetics of CPPL was studied using $^{99\text{m}}\text{Tc}$ -labeled liposomes, and results were compared with that of PL to analyze the circulation characteristics of CPPL in normal rats.

$^{99\text{m}}\text{Tc}$ -labeled CPPL and PL were prepared via postinsertion method (Supplementary materials).¹⁵ Under anesthesia with 10% chloral hydrate, 0.8 mL of $^{99\text{m}}\text{Tc}$ -4%CPPL ($^{99\text{m}}\text{Tc}$ -PL) solution (59.2 MBq/200 g, 8 mg phospholipid/200 g) were injected intravenously to each male Sprague Dawley rat ($n=5$, average weight of 200 g) through the lateral tail vein. Blood samples were collected from the eye at 0.5 hour, 1 hour, 2 hours, 4 hours, 6 hours, 8 hours, 12 hours, and 24 hours. The animal was sacrificed at 24 hours, and the organs of interest were removed and weighed. The amount of radioactivity was measured with an automatic γ -counter (Wallace 1470 Wizard, USA). The percentage dose per gram (% ID/g) of blood or organ was calculated by comparing the counts with 1% aliquot of the injected dose as a standard. The concentration of phospholipid (c , mg/g) was calculated by multiplying the phospholipid dosage (8 mg) with % ID/g. The pharmacokinetic parameters were calculated using WinNonLin software (Version 5.2.1; Pharsight Corporation, St Louis, MO, USA).

To find out the biodistribution of CPPL in BALB/c nude mice bearing breast tumor, 4 mol% CPP-FITC of SPC was used in preparing FITC-CPPL for in vivo organ and tissue images. FITC-CPP-modified PL (FITC-CPL) served as the control group. A total of 200 μL of MCF-7 suspension (1×10^6 cells/mL) was injected into the right armpits of female BALB/c nude mice. These animals were intravenously injected with 200 μL FITC-CPPL at phospholipid dosage of 1 mg/20 g body weight upon reaching a tumor volume of $\sim 200 \text{ mm}^3$. These animals were sacrificed via cervical dislocation at indicated points (2 hours, 4 hours, and 8 hours after injection). Major organs and tissues (eg, heart, liver, spleen, lung, kidney, brain, and tumor) were collected and conducted using Kodak in vivo Imaging System FX PRO (Carestream Health, Inc., USA) with an excitation bandpass filter at 490 nm and emission wavelength of 600 nm. The exposure time was 30 seconds per image. The fluorescent signal intensities were analyzed using Carestream MI SE software.

Statistical analysis

Statistical data were processed using Microsoft Excel 2010 software and SPSS and presented as mean \pm standard deviation (SD) of at least three independent experiments. The differences/correlations between two groups were analyzed using Student's t -test, in which data were considered statistically significant if $P < 0.05$ (*) and very significant if $P < 0.01$ (**).

Results

Characterization of CPPL

For CPP-modified pH-sensitive liposomes, we focused on the optimization of CPP density in order to increase specificity and efficiency of CPP to tumor cells. CPP densities in different CPPL formulations were analyzed to ensure accuracy of the evaluation. As CPP content in CPPL formulations changed from 1 mol% to 8 mol%, *ce* was always ~75%, which indicates that *ce* is a balanced constant and independent of CPP content. Therefore, the quantity of CPP being used during CPPL preparation was calculated by dividing the designed CPP density (eg, 1%, 2%, 4%, and 8%) with *ce* (75%). The exact density of CPP on CPPL could be obtained by removing unreacted CPP from CPPL with ultrafiltering technique described in the *ce* measurement.

The sizes of each liposomes were ~140 nm, while the zeta potential of liposomes changed remarkably after modifications with CPP (Table 1). As compared to PL at pH 7.0, the zeta potential of CPP-modified liposomes increases indicating the effect of positive charges of CPP. At pH 6.0, the zeta potential of CPPL was further increased to a positive value due to the coupling of CPPL with more H⁺ in acidic environment.

pH sensitivity of PHS

PEG was detected by an ELSD detector instead of ultraviolet detector because of its weak ultraviolet absorption.^{16,17} The resolution (R) between PSL (or CL) and PEG exceeded 3.2, representing a satisfactory separation between them (Figure 3A). At pH 7.0, the PEG peak did not appear in PSL, indicating that PSL was stable and PEG could not be cleaved from the liposomes. However, at pH 6.5, 6.0, or 4.5, PEG peaks appeared in HPLC spectrum. The relative masses of PEG under these three pH conditions were ~13.46%, which is equivalent to 7.9 mol% PEG of SPC, indicating that PEG could be completely cleaved from the liposomes (8% PEG in formulation) in 30 minutes when the solution pH is <6.5.

FCM results showed that FI of coumarin-6-PL was lower than that of coumarin-6-CL (without PEG), which demonstrated an attenuated interaction between liposomes and cells caused by the hydration shell of PEG (Figure 3B) on liposomes. And cellular uptake of coumarin-6-CL or coumarin-6-PL was not influenced by pH value. By contrast, coumarin-6 loaded by PSL was sensitive to pH value: FI of coumarin-6-loaded PSL at pH 7.0 and pH 6.0 showed qualitative agreement with that of PL and CL, respectively. The pH sensitivity observed in PSL (Figure 3B) indicated that PEG had been cleaved from PSL completely as a result of Hz degradation at pH 6.0.

Optimization of CPP density on CPPL

Previous results indicate that PEG modification on liposome surface exhibited better long-circulating behavior when PEG density remaining at ~8 mol% of SPC.¹⁸ We screened CPP density using a fixed PEG density at 8%. At pH 6.0, the uptake of coumarin-6-CPPL by MCF-7 cells improved with the increasing of CPP density (Figure 4), as a result of PEG cleaved from liposome surface and internal CPP exposure to promote penetration and endocytosis to the cells. However, under the pH value of 7.0, PEG potentially shielded CPP for a limited extent. The penetration action of CPP at lower density was blocked. When CPP density reached 4%, an increase in cellular uptake of coumarin-6-CPPL was observed (Figure 4). According to the effect of CPP density in CPPL on the uptake of cells at pH 6.0 and 7.0, we confirmed that the optimal density of CPP in the pH-sensitive liposomes is 4%. Under such density, the CPPL carrier is expected to be able to penetrate tumor cells more efficiently; meanwhile, it would not be captured by normal cells and remains circulating in systemic circulation for longer time.

Cell internalization detected with CLSM

DOX is a typical antitumor drug that destroys the structure of DNA in nuclei and emits fluorescence afterward. CLSM results revealed that the distribution of DOX-4%CPPL in

Table 1 Size and zeta potential of liposome influenced by CPP and PEG (mean ± SD, n=3)

Group	Size (nm)	PDI	Zeta potential (mV)
pH 7.0			
PL (containing STR)	138.01±2.64	0.236±0.001	-30.35±1.95
4% CCL	148.75±2.75	0.196±0.01	-0.0061±1.95**
4% CPPL	142.13±4.43	0.252±0.016	-0.0262±0.06**
pH 6.0			
4% CPPL	143.75±1.25	0.189±0.011	0.123±0.02***

Notes: **P<0.01, control group: PL. ***When compared to PL, P<0.01 and when the control group is 4 mol% CPPL at pH 7.0, P<0.05.

Abbreviations: PDI, polydispersity index; PL, PEGylated liposomes; CCL, CPP-modified conventional liposomes; CPPL, CPP-modified pH-sensitive PEGylated liposomes; STR, stearic acid; CPP, cell-penetrating peptide; PEG, polyethylene glycol.

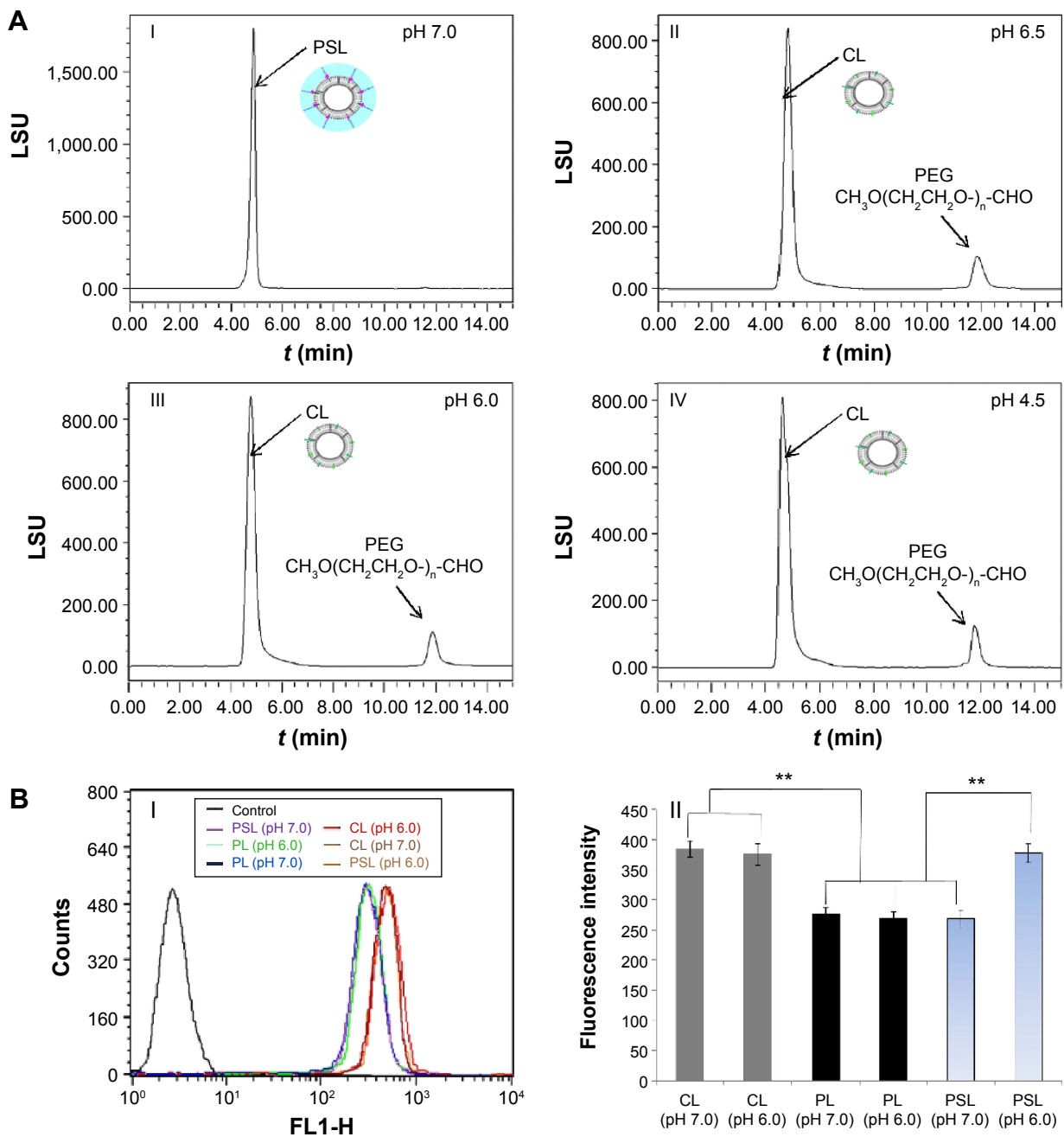


Figure 3 (A) HPLC/ELSD analysis of PEG cleavage from PSL at different pH. (I) pH 7.0, (II) pH 6.5, (III) pH 6.0, (IV) pH 4.5. (B) pH sensitivity of PSL measured with flow cytometer. CL and PL served as control groups. Coumarin-6 was selected as a model drug to indicate the cellular uptake of each liposomal carrier at different pH on MCF-7 cells due to its fluorescence emission ($\lambda_{\text{ex}}=466 \text{ nm}$, $\lambda_{\text{em}}=504 \text{ nm}$ [$n=3$]). ** $P < 0.05$.

Abbreviations: HPLC, high-performance liquid chromatography; CL, conventional liposomes; PL, PEGylated liposomes; PSL, pH-sensitive PEGylated liposomes; PEG, polyethylene glycol; min, minutes.

the cytosol increased 1.6 times compared to DOX-PSL as well as DOX-4%CPPL at pH 6.0 and was correspondent to DOX-CCL (Figure 5A and B). However, under pH 7.0, no significant difference was observed between DOX-4%CPPL and DOX-4%CPL. Such a difference demonstrated that PEG modification on CPPL was quite stable and CPP could be “shielded” well when the pH value was 7.0, but at lower pH (6.0), CPPL promotes more DOX entering into the cells due

to the exposure of CPP on liposome surfaces. The uptake of CPPL was found to be dependent on incubation time only at a pH value of 6.0 (Figure 5C and D), suggesting that the transfection of 4% CPPL-loading DOX was a dynamic process. The longer CPP- H^+ contact cell, the more DOX can be released into cytosol that leads more drugs entering into nuclei and taking actions accordingly. However, due to the barrier of PEG, the cellular uptake of DOX-4%CPPL at

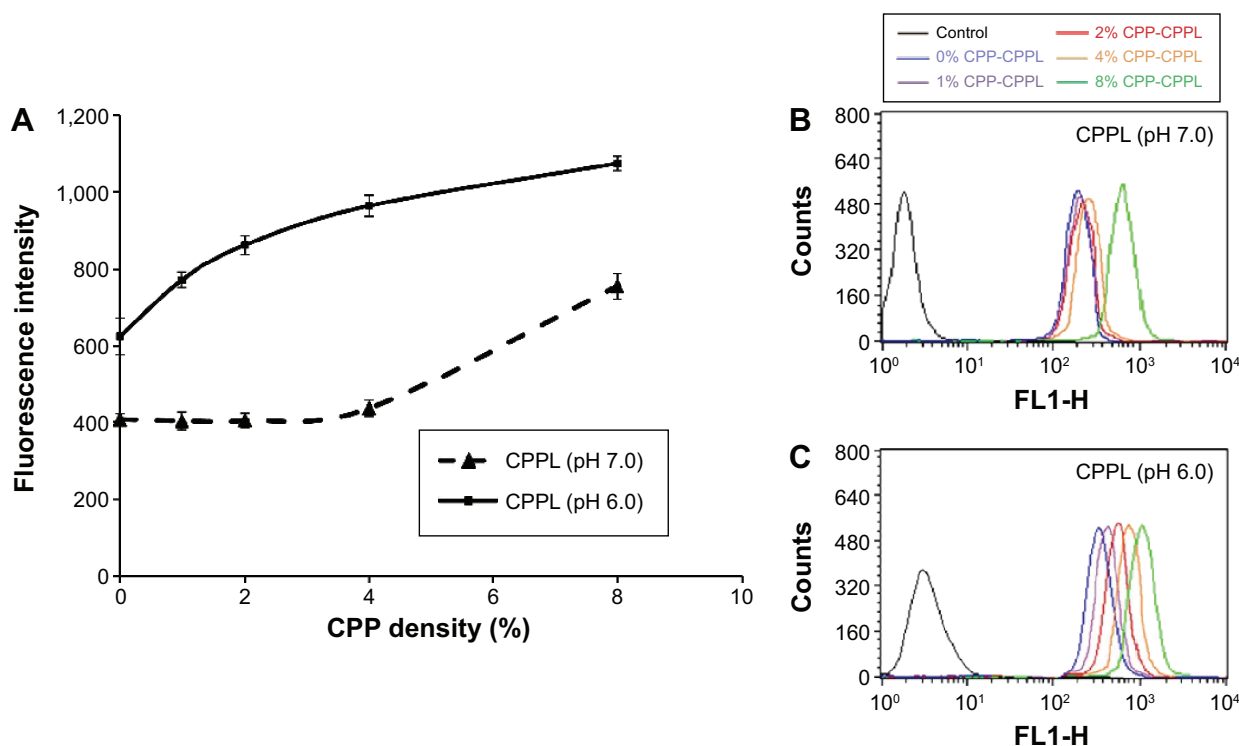


Figure 4 Effect of CPP density on cell uptake of coumarin-6-CPPL at pH 6.0 and 7.0 ($n=3$).

Notes: (A) Effect of CPP density on cell uptake of coumarin-6-CPPL at pH 6.0 and 7.0. (B,C) The cells distribution with fluorescence intensity of CPPL detected by FCM at pH 7.0 and pH 6.0, respectively.

Abbreviations: CPP, cell-penetrating peptide; CPPL, CPP-modified pH-sensitive PEGylated liposomes; PEG, polyethylene glycol.

pH 7.0 stayed same even though the incubation time was prolonged.

Endosomal escape of anticancer drugs loaded by liposomes after tracking into the cell is essential for postdispersing in cytosol and then entering nucleus to inhibit DNA and RNA synthesis.¹⁹ As shown in Figure 6, after 2 hours endosomal escaping, internalized coumarin-6-CPPL distributed more into cytosol of MCF-7 cells than that of coumarin-6-PL. Green fluorescence of coumarin-6 in CPPL was not colocalizing with lysosomes marker (LysoTracker Red) and produced orange color, but coumarin-6-PL preferred to be detained in lysosome and almost completely colocalized with LysoTracker Red to exhibit bright yellow color. The results demonstrated that CPPL might play an additional role in mediating endosomal escape, along with the well-recognized role in enhancing cellular uptake.

Pharmacokinetics and biodistribution of 4% CPPL and PL in vivo

CPPL showed similar long-circulating characteristics as PL in normal rats (Table 2), which demonstrated that CPP is protected by PEG in normal circulation and has potential to play crucial roles for cell penetration in tumor. The tissue distribution in normal rats at 24 hours (Table 3) revealed that

4% CPPL distributed more in liver, less in spleen than PL, but was not distinctly different from PL in heart, lung, kidney, and brain.

DIR is a hydrophobic fluorescent probe that is often used as an imaging agent tracing the distribution of nano-carriers in vivo. However, the fluorescence of DIR is easily quenched in alkaline environment, where CPP is conjugated with activated STR-NHS during the preparation of CPPL. Therefore, CPP-FITC was chosen to prepare FITC-CPPL instead of using CPPL-loaded DIR for image studies on nude mice bearing breast tumor. Since the FI of FITC is too weak to penetrate the animal skin, we directly observed ex vivo image of organs and tissues. CPL was used as a control group due to its pH insensitivity and non-CPP-penetrating function under PEG mask. FITC-CPPL exhibited much stronger signal in tumor than that of FITC-CPL at each time point from various organ images (Figure 7). Ex vivo image of dissected spleen indicated higher fluorescence accumulation in the PL group compared to CPPL. There were no distinct difference between CPPL and PL on the distribution in brain, heart, lung, and kidney. These results were consistent with biodistribution results measured with ^{99m}Tc-labeled liposomes in normal rats. Therefore, ex vivo assay confirmed that 4% CPPL could enhance the targeting efficiency of liposomes

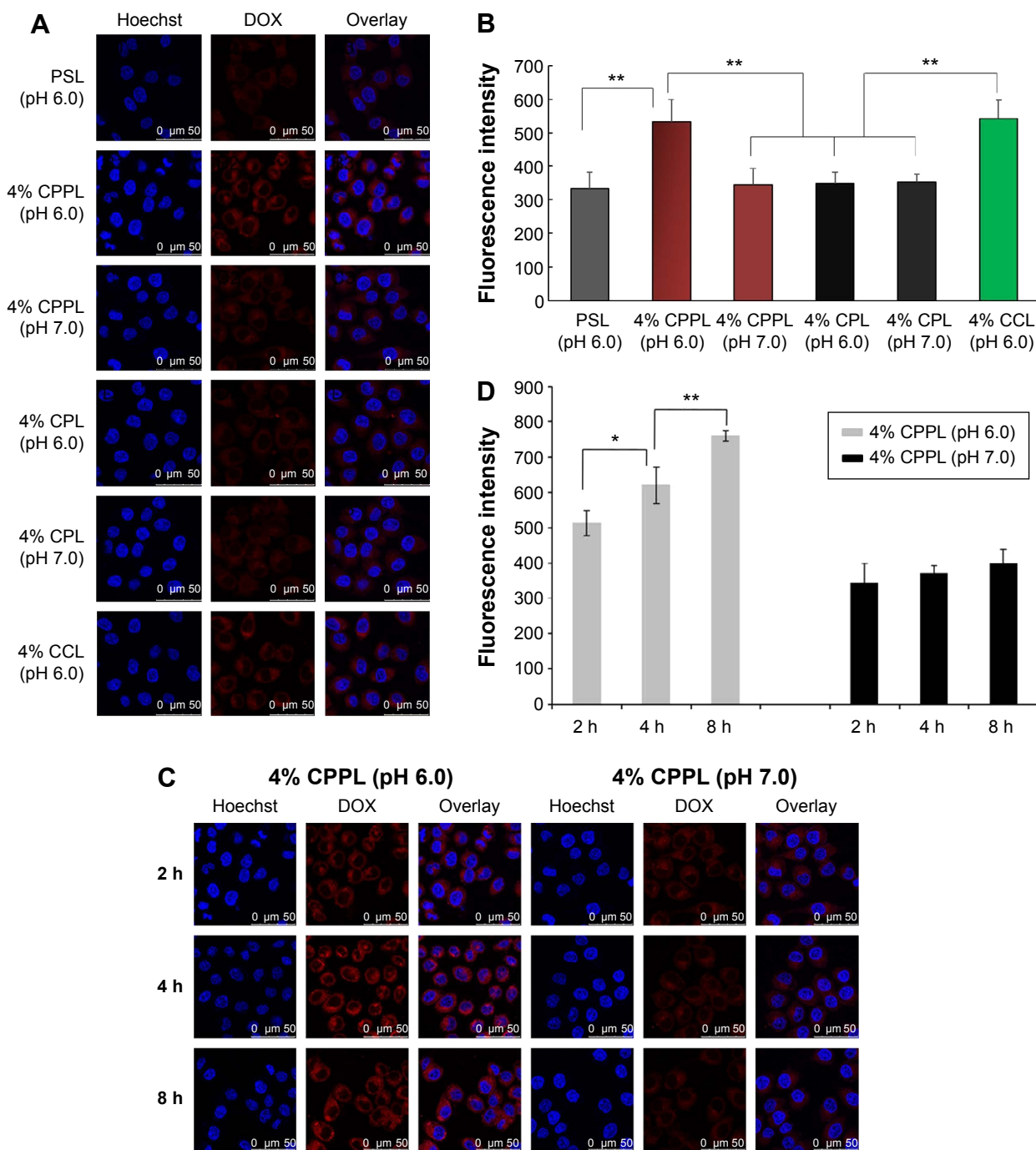


Figure 5 (A) CLSM of DOX loaded with 4% CPP-modified CPPL at different pH. CPL (4% CPP modified, acid-insensitive) and PSL (non-CPP-modified and acid-sensitive) are negative control groups and CCL is served as positive control. (C) Effects of incubation time on cell uptake of DOX loaded by 4% CPPL at pH 6.0 and 7.0. The Hoechst33258 was excited by a 345-nm laser. Those in blue represent the nuclei stained with Hoechst33258, and those in red represent DOX fluorescence ($\lambda_{ex}=480$ nm, $\lambda_{em}=540$ nm). Scale bar is 50 μ m. Quantitative analysis via ImageJ is shown in (B) and (D), * $P<0.05$, ** $P<0.01$ (n=15).

Abbreviations: CLSM, confocal laser-scanning microscope; PSL, pH-sensitive PEGylated liposomes; CPL, CPP-modified PEGylated liposomes; CPPL, CPP-modified pH-sensitive PEGylated liposomes; CCL, CPP-modified conventional liposomes; CPP, cell-penetrating peptide; PEG, polyethylene glycol; DOX, doxorubicin; h, hours.

for breast tumors and reduced the accumulation in normal organs and tissues, especially in spleen.

Discussion

Modifications of liposome surface with PEG derivatives have served as a milestone in the development of liposomes.²⁰

This important strategy could prevent the penetration of CPP toward normal cells by taking the advantage of PEG hydration layer on the surface of liposomes.^{6,7} However, such PEG layer also resembles like a “double-edged sword”. On one hand, it restricted the interaction between PL and opsonin and prolonged the circulation of drug-loaded liposomes in blood.

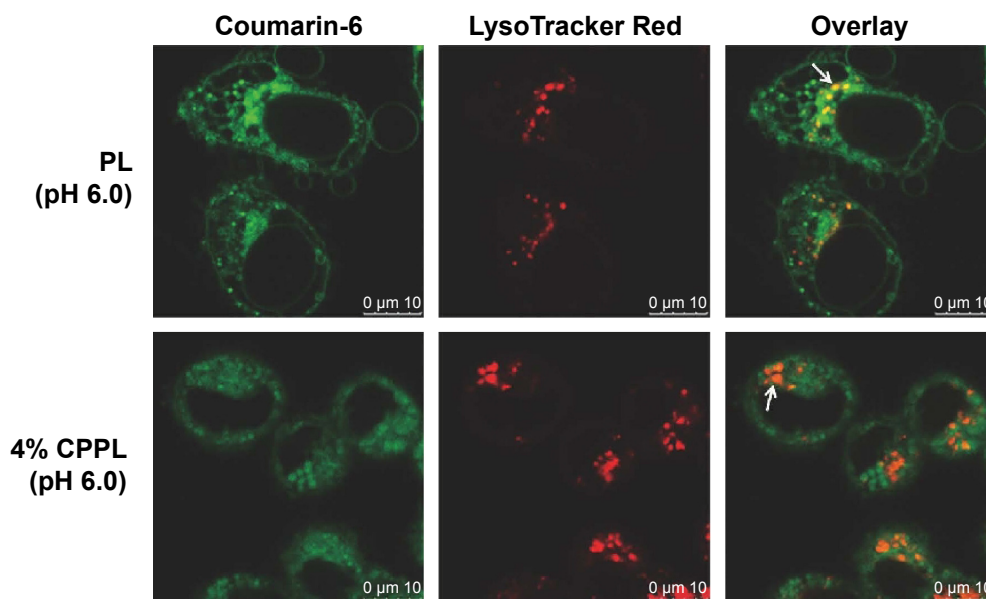


Figure 6 Colocalization of coumarin-6 and lysosomes observed with CLSM after cell internalization with CCPL and endosome escaping for 2 hours. PL is a control group. Co-location description was indicated by the white arrow.

Abbreviations: CLSM, confocal laser-scanning microscope; PL, PEGylated liposomes; CPPL, CPP-modified pH-sensitive PEGylated liposomes; CPP, cell-penetrating peptide; PEG, polyethylene glycol.

On the other hand, it blocked the cellular uptake of liposome when reaching at tumor sites. The layer even reduced “targeting” abilities of the linked ligand toward liposomes and further lowered the efficiency of targeted delivery.²¹ In this work, we synthesized a new PEG derivative PHS and prepared a pH-sensitive liposomes that provided possibility for PEG to accomplish its perfect dialectical unification under both normal and tumor environment.

Both HPLC and FCM methods confirmed that PHS has a distinct acid sensitivity in comparison with PEG2000-Hz-PE.⁷ PEG2000-Hz-PE conjugate exhibited a degradation half-time of 3.0 hours at pH 5.5; however, the Hz bond in PHS was completely cleaved within 30 minutes at pH 6.5. The stronger acid sensitivity of PHS results from the presence

of a methylene group (electron donating) (Figure 1) next to the hydrazine bond that could facilitate hydration under mild acidic conditions. On the contrary, an immediate aromatic ring (electron withdrawing)⁷ next to hydrazone bond in PEG2000-Hz-PE weakens the hydrolysis effect. Such a difference in pH sensitivity promised that CPP could penetrate cells in a timely manner as soon as CPPL arrives at tumor site. Another advantage of using PHS lies in its higher insertion efficiency into liposomes judged by its higher critical micelle concentration (CMC). The CMC of PEG2000-PE and PHS, which were measured with pyrene probe, is 8.57×10^{-6} mol/L and 1.23×10^{-4} mol/L, respectively (Supplementary materials). Since the higher the CMC is, the more difficult micelles form, PHS in solutions is prone to be inserted into liposomes rather than forming micelles.²²

Table 2 Pharmacokinetic parameters of ^{99m}Tc -CPPL and ^{99m}Tc -PL (mean \pm SD, n=5)

Parameter	Unit	CPPL	PL
C_0	mg/mL	0.24 \pm 0.04	0.25 \pm 0.04
$t_{1/2}(\alpha)$	min	25.93 \pm 11.98	22.59 \pm 13.86
$t_{1/2}(\beta)$	min	667.11 \pm 202.92	539.70 \pm 122.28
AUC	min·mg·mL ⁻¹	77.31 \pm 23.16	111.14 \pm 17.856
Cl	mL·h ⁻¹	6.67 \pm 1.97	4.45 \pm 0.01
K_{10}	min ⁻¹	0.06 \pm 0.01	0.09 \pm 0.02
V _{ss}	mL	93.32 \pm 17.24	54.14 \pm 3.92
AUMC	min ² ·mg·mL ⁻¹	72,863.71 \pm 4,254.66	86,408.20 \pm 3,163.93
MRT	min	887.25 \pm 257.16	756.95 \pm 165.22

Abbreviations: PL, PEGylated liposomes; CPPL, CPP-modified pH-sensitive PEGylated liposomes; AUC, area under the curve.

Table 3 Biodistribution of ^{99m}Tc -CPPL and ^{99m}Tc -PL in normal rats for 24 hours (mean \pm SD, n=5)

Tissue	PL ($\mu\text{g/g}$)	CPPL ($\mu\text{g/g}$)
Heart	4.62 \pm 1.50	10.54 \pm 3.22
Liver	74.91 \pm 13.20	260.69 \pm 89.01*
Spleen	1,470.52 \pm 115.7	594.24 \pm 189.33*
Lung	12.32 \pm 4.81	27.31 \pm 9.91
Kidney	29.49 \pm 9.5	60.89 \pm 14.36
Brain	0.61 \pm 0.01	1.01 \pm 0.35

Note: * $P < 0.05$, CPPL vs PL.

Abbreviations: PL, PEGylated liposomes; CPPL, CPP-modified pH-sensitive PEGylated liposomes; PEG, polyethylene glycol.

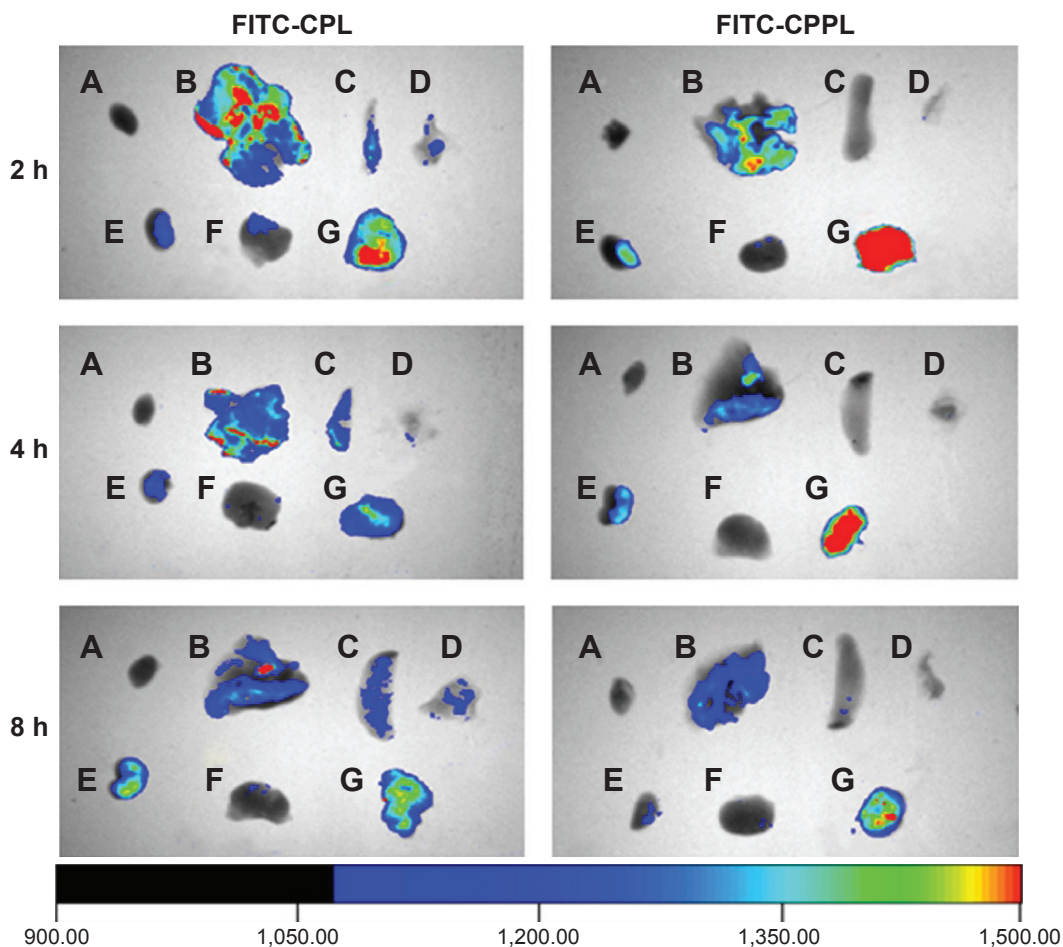


Figure 7 Ex vivo images of interested organs after 2 hours, 4 hours, and 8 hours intravenous administrated FITC-CPPL and FITC-CPL in tumor-bearing nude mice.

Notes: (A) Heart, (B) liver, (C) spleen, (D) lung, (E) kidney, (F) brain, and (G) tumor (from left to right).

Abbreviations: CPL, CPP-modified PEGylated liposomes; CPPL, CPP-modified pH-sensitive PEGylated liposomes; CPP, cell-penetrating peptide; PEG, polyethylene glycol; h, hours.

The penetrating ability of CPP is related to its positive charges.⁴ Until now, no work has reported the relationship between the CPP content and its penetrating function. In general, 2 mol% CPP density was chosen in most DDS penetration,⁶ but it lacks the basis. In the current work, we are the first one to optimize CPP density for the purpose of improving specificity and efficiency of CPP in tumor cells. We discovered that the optimal density of CPP is 4 mol% of lipid.

Pharmacokinetics results in normal rats showed similar long-circulating characteristics of CPPL as that of PL, which proved that CPP was protected by PEG in normal circulation and CPPL has great potential to penetrate tumor cells under acidic condition. It was reported that CPP-modified sterically stabilized liposomes (CPP-SSL), in which CPP was coupled with the distal end of PL, were quickly cleared from blood due to its penetrating ability to normal tissues.⁹ Our novel CPPL carrier could solve the problem of high blood clearance since the position of CPP on liposomes is different from that of CPP-SSL.

It is well known that normal blood remains well-buffered and constant pH of 7.0–7.4, while extracellular pH of most solid tumors ranges from pH 6.5 to 7.2, and it approaches to 6.0 when tumor grows exceedingly fast. Moreover, pH can drop as low as 5.5–6.0 in endosomes and 4.5–5.0 in lysosomes.²³ In this regard, CPPL containing PHS constitutes a promising strategy to improve tumor selectivity of CPP since liposomes are stable at physiological pH but undergo PEG departing from liposomes under acidic conditions, thus leading to an efficient exposure of CPP peptides on the surface of liposomes to penetrate the membrane of tumor cells. When trapped in endosomes after uptake, CPL adsorbs more H⁺ and then promotes the lipid fusion between cationic CPP-H⁺ liposomes and anionic components in the endosomal membrane via electronic attraction. Fusion pore is subsequently formed for releasing the liposomal cargoes into the cytosol.¹⁹ Entrapped cargoes, such as DOX, gain more opportunities entering nucleus to exert pharmacological effects. The presence of PEG chains on liposomes

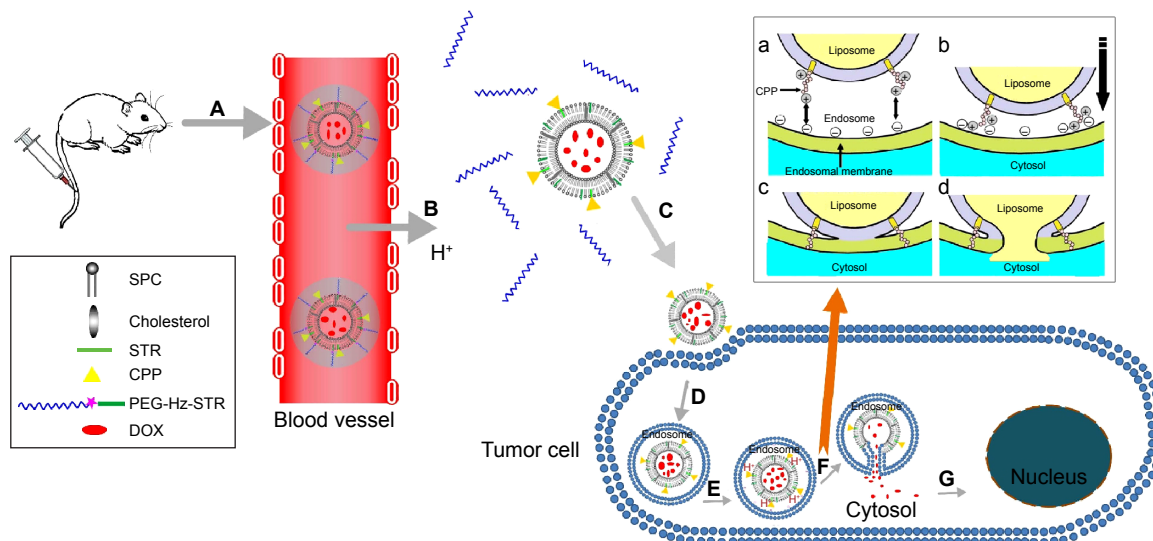


Figure 8 Scheme of CPPL in vivo tumor targeting process.

Notes: (A) PEG was kept on the surface of CPPL in the neutral environment of blood. (B) CPPL accumulated at the tumor site via EPR effect, and then CPP was exposed on the surface of liposomes as a result of the missing of PEG caused by the degradation of hydrazone bond at low pH tumor area. (C) Improved cellular uptake due to the exposed CPP. (D) Internalization of CCL into tumor cells. (E) CPP adsorbed more H^+ in endosome. (E) CPP adsorbed more H^+ in endosome and Electrostatic attraction between the cationic CPP- H^+ and the anionic components in the endosomal membrane happened. (F) Fusion pore formed and the liposomal cargo was released into the cytosol. (G) The released cargoes has more opportunity entering into nuclei.

Abbreviations: PEG, polyethylene glycol; CPP, cell-penetrating peptide; CPPL, CPP-modified pH-sensitive PEGylated liposomes; EPR, enhanced permeability and retention; CCL, CPP-modified conventional liposomes; CPP, cell-penetrating peptide; SPC, soybean phosphatidylcholine; STR, stearic acid; DOX, doxorubicin.

may prevent the fusion between the two membranes due to its steric hindrance caused by the bulky hydrophilic PEG chains.²⁴ Since PEG was removed from the lipid bilayer prior to or just after cellular uptake, CPPL performed further advantage in the formation of fusion pore for endosomal escaping. In vivo the transporting process of CPPL-loaded DOX was illustrated in Figure 8.

Herein, we constructed a novel type of pH-sensitive PSL to improve CPP's selectivity toward tumors and optimized CPP density to maximize cell penetration efficiency at tumor sites. Such a simple and efficient CPPL DDS demonstrated long blood circulation in vivo, specific tumor targeting, as well as high cell-penetrating and endosomal escape abilities, which accomplished our goal of targeting subcellular compartments and identifying potential antitumor drug carriers in clinical applications.

Conclusion

We constructed a novel kind of PSL to improve CPP selectivity toward tumors and optimized CPP density to maximize cell penetration efficiency at tumor sites. Such simple and efficient CPPL DDS demonstrates long blood circulation in vivo, specific tumor targeting, as well as high cell-penetrating and endosomal escape abilities, which accomplished the goal of targeting subcellular compartments and identifying potential antitumor drug carriers in clinical applications.

Highlight

- A new PEG derivative by conjugating PEG with STR via acid-degradable hydrazone bond (PEG2000-Hz-STR, PHS) showed stronger pH sensitivity than that of PEG2000-Hz-PE.
- CPPs were directly attached to liposome surfaces via coupling with STR to avoid the hindrance of PEG as a linker on the penetrating efficiency of CPP.
- An optimal CPP density on liposomes was screened to guaranty a maximum targeting efficiency on tumor cells as well as not being captured by normal cells that resulted in a long circulation in blood.
- FCM and CLSM experiments confirmed that novel CPPL exhibited superior capability in cellular uptake and endosomal escaping. Pharmacokinetics in normal Sprague Dawley rat revealed that CPPL have overcome accelerate blood clearance that was induced by the direct exposure of CPP on liposomes.

Acknowledgments

This work was supported by the National Natural Science Foundation of China (Grant No 81202469). The authors would like to thank Professor Hongmei Jia and Dr Jie Lu from Beijing Normal University for generously providing HYNIC and $SnCl_2$ -Tricine kits for labeling liposomes with ^{99m}Tc .

Disclosure

The authors report no conflicts of interest in this work.

References

1. Cullis PR, Chonn A. Recent advances in liposome technologies and their applications for systemic gene delivery. *Adv Drug Deliv Rev.* 1998;30(1-3):73-83.
2. Biswas S, Dodwadkar NS, Piroyan A, Torchilin VP. Surface conjugation of triphenylphosphonium to target poly(amidoamine) dendrimers to mitochondria. *Biomaterials.* 2012;33(18):4773-4782.
3. Zhou J, Zhao WY, Ma X, et al. The anticancer efficacy of paclitaxel liposomes modified with mitochondrial targeting conjugate in resistant lung cancer. *Biomaterials.* 2013;34(14):3626-3638.
4. Koren E, Torchilin VP. Cell-penetrating peptides: breaking through to the other side. *Trends Mol Med.* 2012;18(7):385-393.
5. Mai JC, Shen H, Watkins SC, Cheng T, Robbins PD. Efficiency of protein transduction is cell type-dependent and is enhanced by dextran sulfate. *J Biol Chem.* 2002;277(33):30208-30218.
6. Koren E, Apte A, Jani A, Torchilin VP. Multifunctional PEGylated 2C5-immunoliposomes containing pH-sensitive bonds and TAT peptide for enhanced tumor cell internalization and cytotoxicity. *J Control Release.* 2012;160(2):264-273.
7. Kale AA, Torchilin VP. "Smart" drug carriers: PEGylated TATp-modified pH-sensitive liposomes. *J Liposome Res.* 2007;17(3-4):197-203.
8. Tu YF, Liu C, Ju R, Xie Y. In vivo study on pharmacokinetics and pharmacodynamics of P167 modified liposomal doxorubicin in rats. *China J Clin Pharm.* 2014;23(1):9-14.
9. Kale AA, Torchilin VP. Design, synthesis, and characterization of pH-sensitive PEG-PE conjugates for stimuli-sensitive pharmaceutical nanocarriers: the effect of substitutes at the hydrazone linkage on the pH stability of PEG-PE conjugates. *Bioconjug Chem.* 2007;18(2):363-370.
10. Maruyama K, Takizawa T, Takahashi N, Tagawa T, Nagaike K, Iwatsuru M. Targeting efficiency of PEG-immunoliposome-conjugated antibodies at PEG terminals. *Adv Drug Deliv Rev.* 1997;24(2-3):235-242.
11. Staros JV. N-hydroxysulfosuccinimide active esters: bis(N-hydroxysulfosuccinimide) esters of two dicarboxylic acids are hydrophilic, membrane-impermeant, protein cross-linkers. *Biochemistry.* 1982;21(17):3950-3955.
12. Yu KF, Zhang WQ, Luo LM, et al. The antitumor activity of a doxorubicin loaded, iRGD-modified sterically-stabilized liposome on B16-F10 melanoma cells: in vitro and in vivo evaluation. *Int J Nanomedicine.* 2013;8:2473-2485.
13. Goins B, Phillips WT, Klipper R. Blood-pool imaging using technetium-99m-labeled liposomes. *J Nucl Med.* 1996;37(8):1374-1379.
14. Karczmarczyk U, Markiewicz A, Mikolajczak R, et al. (99m)Tc human IgG radiolabelled by HYNIC. Biodistribution and scintigraphy of experimentally induced inflammatory lesions in animal model. *Nucl Med Rev Cent East Eur.* 2004;7(2):107-112.
15. Laverman P, Dams ET, Oyen WJ, et al. A novel method to label liposomes with 99mTc by the hydrazino nicotinyl derivative. *J Nucl Med.* 1999;40(1):192-197.
16. Lee YH, Jeong ES, Cho HE, Moon DC. Separation and determination of polyethylene glycol fatty acid esters in cosmetics by a reversed-phase HPLC/ELSD. *Talanta.* 2008;4(5):1615-1620.
17. Shibata H, Yomota C, Okuda H. Simultaneous determination of polyethylene glycol-conjugated liposome components by using reversed-phase high-performance liquid chromatography with UV and evaporative light scattering detection. *AAPS PharmSciTech.* 2013;14(2):811-817.
18. Xiong XB, Huang Y, Lu WL, et al. Intracellular delivery of doxorubicin with RGD-modified sterically stabilized liposomes for an improved antitumor efficacy: in vitro and in vivo. *J Pharm Sci.* 2005;94(8):1782-1793.
19. El-Sayed A, Futaki S, Harashima H. Delivery of macromolecules using arginine-rich cell-penetrating peptides: ways to overcome endosomal entrapment. *AAPS J.* 2009;11(1):13-22.
20. Barenholz Y. Doxil(R) – the first FDA-approved nano-drug: lessons learned. *J Control Release.* 2012;160(2):117-134.
21. Mori A, Klivanov AL, Torchilin VP, Huang L. Influence of the steric barrier activity of amphiphatic poly (ethyleneglycol) and ganglioside GM1 on the circulation time of liposomes and the target binding of immunoliposomes in vivo. *FEBS Lett.* 1991;284(2):263-266.
22. Xie Y, Ye L, Zhang XB, et al. Transport of nerve growth factor encapsulated into liposomes across the blood-brain barrier: in vitro and in vivo studies. *J Control Release.* 2005;105(1-2):106-119.
23. Yin H, Lee ES, Oh KT, Kim DI, Bae YH. Physicochemical properties of pH sensitive poly(L-histidine)-b-poly(ethylene glycol)/poly(L-lactide)-b-poly(-ethylene glycol) mixed micelles. *J Control Release.* 2008;126(2):130-138.
24. Holland JW, Hui C, Cullis PR, Madden TD. Poly(ethylene glycol)-lipid conjugates regulate the calcium-induced fusion of liposomes composed of phosphatidylethanolamine and phosphatidylserine. *Biochemistry.* 1996;35(8):2618-2624.

Supplementary materials

Effect of polyethylene glycol coupled with cell-penetrating peptide in liposomes on cellular uptake

Preparation and evaluation of CPP-modified sterically stabilized liposomes

First, 1,2-distearoyl-sn-glycero-3-phosphoethanolamine-*N*-[methoxy(polyethyleneglycol)-2000]-cell-penetrating peptide (DSPE-PEG2000-CPP) conjugate was synthesized and purified according to an established procedure with some modifications.¹ CPP was reacted with a 1.2-fold molar excess of DSPE-PEG2000-NHS in dimethyl formamide with the presence of minute quantity of triethylamine. The reaction mixture was stirred overnight at 25°C and then dialyzed against deionized water using a cellulose ester membrane filter (MWCO, 3,500 Da) till unreacted CPP was removed. The product was identified by MALDI-TOF-MS (Figure S1) after being freeze-dried.

Then, CPP-modified sterically stabilized liposomes (CPP-SSL) were prepared by thin film hydration method:² soybean phosphatidylcholine (SPC):cholesterol:DSPE-PEG2000:DSPE-PEG2000-CPP (100:50:5:3) were dissolved in a mixture of chloroform:methanol (4:1 v/v), and solvent was evaporated under reduced pressure. The thin film was hydrated with phosphate-buffered saline (pH 7.0) under sonication at 37°C for 20 minutes to form CPP-SSL.

The coupling efficient (*ce*) of CPP on the liposomes was determined by super filter method described in the preparation of CPP-modified pH-sensitive PEGylated liposomes (CPPL) to be ~95%.

Comparison of CPPL and CPP-SSL on cellular uptake of coumarin-6

Flow cytometry was used to determine the cellular uptake of coumarin-6 loaded by CPPL and CPP-SSL in which terminal CPP density was 4%. PL served as a control group. MCF-7 cells were incubated with free serum RPMI 1640 containing 100 ng/mL coumarin-6 loaded by CPPL, CPP-SSL, and PL at pH 6.0 for 3 hours. Fluorescence intensities of each sample were measured by a flow meter based on the protocol of flow cytometry and were shown in Figure S2. Fluorescence intensities of CPP-SSL and CPPL were approximately 1.95 and 2.40 times higher than that of PL, indicating that CPP were able to penetrate cells when either directly coupled with liposomes or conjugated with the distal end of PEG in liposomes. Furthermore, lower CPP-SSL cellular uptake of coumarin-6 than CPPL demonstrated that conjugation of CPP with PEG could prevent the penetrating abilities of CPP.

Synthesis of PHS (mPEG2000-hydrazone-STR)

First, mPEG2000-Hz-PDP was synthesized by stirring mPEG2000-CHO with 3-(2-pyridyldithio)propionylhydrazide

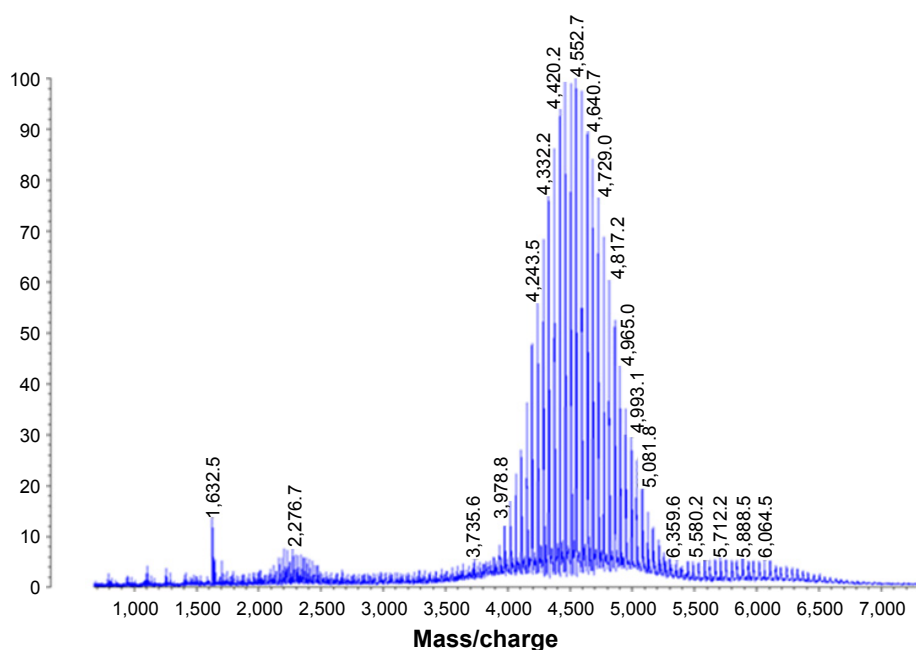


Figure S1 MALDI-TOF-MS of DSPE-PEG2000-CPP.

Notes: The molecular weight distribution indicated that CPP was conjugated with the distal end of PEG at 1:1 molar ratio to form the conjugate of DSPE-PEG-CPP7.

Abbreviations: PEG, polyethylene glycol; CPP, cell-penetrating peptide.

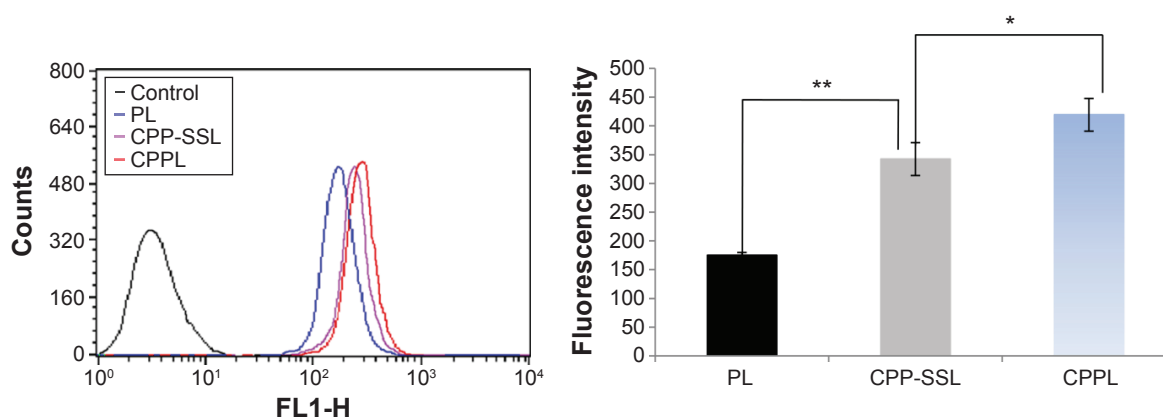


Figure S2 Effect of PEG coupled with CPP in liposomes on cellular uptake measured with flow cytometry analysis.

Notes: PL served as control groups. Coumarin-6 was selected as a model drug to indicate cellular uptake ability of each liposomal carrier at pH 6.0 on MCF-7 cells due to its fluorescence ($\lambda_{ex}=466$ nm, $\lambda_{em}=504$ nm [n=3]). * $P<0.05$, ** $P<0.01$.

Abbreviations: PEG, polyethylene glycol; CPP, cell-penetrating peptide; PL, PEGylated liposomes; CPP-SSL, CPP-modified sterically stabilized liposomes; CPPL, CPP-modified PEGylated liposomes.

in chloroform under argon gas protection for 48 hours at room temperature. STR-SH was then dissolved in anhydrous chloroform containing mPEG2000-Hz-PDP in the presence of triethylamine. The mixture was stirred under argon gas environment for 24 hours. Chloroform was evaporated under reduced pressure, and the conjugate was purified by size exclusion gel chromatography using Sepharose CL-4B media. White powder of the product was obtained after freeze-drying.

Preparation of ^{99m}Tc -labeled CPPL and PL

DSPE-HYNIC was first synthesized by stirring 1.28 μmol DSPE, 7 μmol S-HYNIC, and 36 μmol triethylamine in 500 μL chloroform at 55°C for 1 hour. SPC/DSPE-HYNIC/cholesterol (2/0.07/1, mol/mol/mol) and 4 mol% CPP of SPC were used to prepare HYNIC-CPPL and HYNIC-PL according to the protocol described in the preparation of CPPL.

The mixture was centrifuged in an ultrafilter tube (MWCO, 30,000 Da) at 10,000 $\times g$ for 30 minutes to remove unreacted HYNIC. HYNIC-CPPL and HYNIC-PL were reacted with $\text{Na } ^{99m}\text{TcO}_4$ solution containing tricine and SnCl_2 at 50°C for 30 minutes, respectively. ^{99m}Tc -labeled liposomes were separated from free $^{99m}\text{TcO}_4^-$ by PD-10 column. The labeling percentage of the liposomes was approximately 16%–20% from the elution curve.

CMC determinations for PHS and DSPE-PEG2000

Since Kalyanasundaram and Thomas³ proved that the characteristic dependence of fluorescence vibrational fine structure of pyrene could be used to determine the critical micelle concentrations (CMCs) of surfactant solutions, the so-called pyrene 1:3 ratio method has become one of the most popular procedures for CMC determinations in micelle

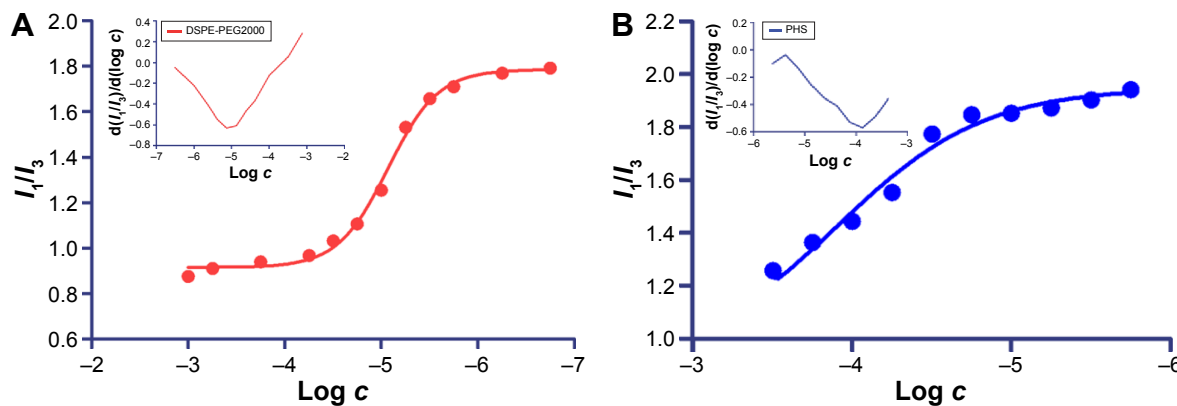


Figure S3 The relationship between I_1/I_3 of pyrene and the concentration of polymer.

Note: CMC is defined as the concentration of polymer corresponding to the inflection point in the curve. When micelle formed, the value of I_1/I_3 decreased significantly with the increase of concentration of polymer. CMC is a value of concentration sudden changed with I_1/I_3 and it was obtained by utilizing the method of partial differential.

Abbreviations: CMC, critical micelle concentration; PEG, polyethylene glycol; PHS, mPEG2000-hydrazone-stearate (mPEG2000-Hz-STR).

systems. For surfactants with very low CMCs (typically below 1×10^{-3} mol/L), CMC values can be obtained from the inflection point of the pyrene 1:3 ratio plots, which is the extremum value from the plot of $d(I_1/I_3)/d(\log c)$ against $\log c$.⁴

Pyrene in acetone was added into a series of 5 mL vials, and solvents were evaporated naturally to obtain dry crystals (6×10^{-9} mol). A 5 mL PHS or DSPE-PEG2000 was added into each vial at a final concentration of 5.62×10^{-3} – 1.00×10^{-7} mol/L. Mixtures were sonicated for 30 minutes at room temperature to completely dissolve pyrene into the medium. Fluorescence emission of a number of surfactant solutions containing 6×10^{-9} mol of pyrene was recorded using an excitation wavelength of 335 nm, and the intensities I_1 and I_3 were measured at the wavelengths corresponding to the first and third vibronic bands located near 373 nm and 384 nm. The ratio I_1/I_3 is the so-called pyrene 1:3 ratio. All fluorescence measurements were carried out

at $25.0^\circ\text{C} \pm 0.1^\circ\text{C}$ with Shimadzu RF-5301PC spectrofluorometer (Japan).

Figure S3 showed I_1/I_3 ratio against surfactant concentration. CMC of PHS and DSPE-PEG2000 was 1.23×10^{-4} mol/L and 8.57×10^{-6} mol/L, respectively.

References

1. Koren E, Apte A, Jani A, Torchilin VP. Multifunctional PEGylated 2C5-immunoliposomes containing pH-sensitive bonds and TAT peptide for enhanced tumor cell internalization and cytotoxicity. *J Control Release*. 2012;160(2):264–273.
2. Chiu SJ, Liu S, Perrotti D, Marcucci G, Lee RJ. Efficient delivery of a Bcl-2-specific antisense oligodeoxyribonucleotide (G3139) via transferrin receptor-targeted liposomes. *J Control Release*. 2006;112(2):199–207.
3. Kalyanasundaram K, Thomas JK. Environmental effects on vibronic band intensities in pyrene monomer fluorescence and their application in studies of micellar systems. *J Am Chem Soc*. 1977;99(7):2039–2044.
4. Aguiar J, Carpena P, Molina-Bolivar JA, Camero Ruiz C. On the determination of the critical micelle concentration by the pyrene 1:3 ratio method. *J Colloid Interface Sci*. 2003;258(1):116–122.

International Journal of Nanomedicine

Publish your work in this journal

The International Journal of Nanomedicine is an international, peer-reviewed journal focusing on the application of nanotechnology in diagnostics, therapeutics, and drug delivery systems throughout the biomedical field. This journal is indexed on PubMed Central, MedLine, CAS, SciSearch®, Current Contents®/Clinical Medicine,

Submit your manuscript here: <http://www.dovepress.com/international-journal-of-nanomedicine-journal>

Dovepress

Journal Citation Reports/Science Edition, EMBase, Scopus and the Elsevier Bibliographic databases. The manuscript management system is completely online and includes a very quick and fair peer-review system, which is all easy to use. Visit <http://www.dovepress.com/testimonials.php> to read real quotes from published authors.